



RESEARCH ARTICLE

A KINETIC STUDY OF THERMOCHEMICALLY BORIDED AISI 316L STAINLESS STEEL

Gökhan BAŞMAN¹, Mustafa Merih ARIKAN^{2,*}, C. Fahir ARISOY³, M. Kelami ŞEŞEN⁴

¹Eti Krom A.Ş., R&D Center, Bingöl Karayolu, 55. Km, Elazığ, gbasman@gmail.com, ORCID: 0000-0001-8835-3641

²*Arikan Engineering and Consultancy, Antalya, meriharikan@yahoo.com, ORCID: 0000-0002-5820-1871

³İstanbul Teknik Üniversitesi, Kimya-Metalurji Fakültesi, Metalurji ve Malzeme Mühendisliği Bölümü, İstanbul, fahir@itu.edu.tr, ORCID: 0000-0003-3399-9271

⁴İstanbul Teknik Üniversitesi, Kimya-Metalurji Fakültesi, Metalurji ve Malzeme Mühendisliği Bölümü, İstanbul, mksesen@itu.edu.tr, ORCID: 0000-0002-8113-6289

Receive Date: 23.03.2022

Accepted Date: 28.03.2023

ABSTRACT

Biomaterials are used in different parts of human body as replacement implants in medical applications. An implant material should have high biocompatibility, corrosion and wear resistance, and suitable mechanical properties in terms of safety and long-service period. There are only a few biocompatible implant materials: AISI316L stainless steel is one of the materials used in this type of applications. They have relatively poor wear resistance. Boriding being a thermochemical diffusion treatment is one of the processes to improve their wear resistance. Borides are formed by introducing boron atoms by diffusion onto a substrate surface and they are non-oxide ceramics and could be very brittle. The growth kinetics of boride layer is analyzed by measuring depth of layers as a function of boriding time within a temperature range. In this study, the effects of Ekabor-2 bath on formation mechanism and properties of boride layer in thermochemical diffusion boriding of AISI316L stainless steel were investigated. Different temperatures and durations were applied in boriding operations and hardness, optical microscopy, XRD, EPMA and SEM studies were performed to detect the properties of boride layers. It was found that thickness of boride layer increased with increasing temperature and time; the basic phase in the boride layer formed was Fe₂B and FeB phase also formed. It was also found that surface hardness values of borided materials increased depending on temperature and time of boriding process; surface hardness values of borided materials are approximately 10 times higher than surface hardness values of non-borided AISI316L stainless steel and formation activation energy of boride layer is 149.3 kJmol⁻¹.

Keywords: *Boriding, AISI 316L Stainless Steel, Diffusion Kinetics, Surface Treatment, Hardness.*

1. INTRODUCTION

Implant materials are internally or externally used in the human body for the cure and repair purposes; this type of materials can be temporary or permanent in the body [1-3]. Biomaterials are used in

different parts of the human body as replacement implants [4-6] and improve the life quality and help increasing the lifetime of human beings. Biomedical implants encompass cardiovascular implantable, neural and orthopedic fixation devices, cochlear and retinal applications, orthopedic prostheses, bone tissue engineering scaffolds and dental implants [7,8]. A metallic implant should possess high biocompatibility, corrosion and wear resistance, and suitable mechanical properties in terms of safety and long service period [9].

There are only a few biocompatible implant materials although the large number of metals and alloys are produced in industry. These materials can be categorized as stainless steels, cobalt-based alloys, titanium-based alloys and the others [5, 10-12].

AISI 316L type stainless steels are used in the applications requiring wear, corrosion and fatigue resistance. 316L stainless steel has a Young Modulus of about 200 GPa, a tensile strength of 500–1000 MPa, and a fracture toughness of $100 \text{ MPa(m)}^{1/2}$ [13] and is used as an implant material to make internal fixation devices and/or prostheses for the amputees due to its good mechanical properties and corrosion resistance, satisfactory biocompatibility and low cost [6,14].

Boriding is one of the processes applied onto the parts made of AISI 316L stainless steels since they have relatively poor wear resistance. A number of surface treatments such as nitriding by ion implantation, pulsed plasma nitriding and plasma immersion ion implantation are also applied to improve their wear resistance without compromising their corrosion resistance [15].

Boriding process is used to increase the hardness, wear, erosion and corrosion resistance on the surfaces of the metals and alloys; and it is also aimed to sustain these properties at elevated temperatures. Boriding process is industrially applied to mostly ferrous-based alloys [16-18]. Boriding is a process in which a boride layer is formed on the surface of the substrate metal by the diffusion of boron atoms at elevated temperatures [15,16,19]. Boriding is also known as the diffusion of boron atoms which will form a compound on the surface. Boriding can be applied to well surface cleaned materials with durations of 1-10 hours at temperatures of 800-1100°C in the various environments such as solid, paste, liquid and gas.

New techniques such as plasma boriding and fluidized bed boriding are also used except for the thermo-chemical boriding methods in the gaseous environment by the technological developments. Non-thermo-chemical physical vapor deposition (PVD), chemical vapor deposition (CVD), plasma-spray and ion deposition are also methods used for boriding [16,20]. Thermo-chemical methods are the most common methods within these techniques. Thermo-chemical boron coating is a method based on the diffusion of boron atoms onto metal as a function of temperature and time.

The most important feature of boriding is that the obtained boride layer has high hardness (1450-5000HV) and high melting temperature. The hardness of the coating layer is permanent up to the lower-critical temperature (650°C) in the ferrous-based materials [21]. The hardness of the boride layers formed on the plain-carbon steels are much higher than the hardness obtained by the cementation and nitration which are traditional hardening methods. Surface hardness values of tool

steels hardened by boriding can reach hardness values of electrolytic hard chromium coating and tungsten carbide.

Boride phase on the surface of material initially grows as nucleus when the iron and ferrous-based materials are borided. Boride layer consists of two different boride layers including (Fe,M)B phase at the outer surface and (Fe,M)₂B phase at the inner part (just above the substrate).

Boride layers in different structures can be obtained by various boriding methods. The structure of boride layers can be either in a smooth form or tooth-shaped morphology depending on the boriding method and the composition of the material to be borided. Determination of some of the layer properties is possible originating from the layer types. Single-phase boride layer (Fe₂B) is preferred in the industry [22]. Post-boriding processes can be applied to the substrate material without affecting the properties of borided layer negatively [20]. It should be taken into consideration that the layer thickness should not be too thick especially on the double-phase layers since brittleness will increase as the layer thickness increase. Boron diffusion into steel becomes more difficult as the content of alloying elements increases [23].

In addition, tooth-shaped boride morphology on the high-alloy steels is denser, more uniform and has a smooth structure. Difficulties arise in the description of the layer thickness and different descriptions are made since the boride layers are in needle or variable form. Layer thickness is given in the literature by comparing the tooth structure to a flat plane and taking the average value of the heights of these teeth according to the plane [16].

Borided steels are characterized by high surface hardness and wear resistance. Another superiority of borided surfaces in terms of wear is that the heat resulting from both working environment and sliding friction does not cause a significant decrease in the hardness and wear resistance of the boride layers [24]. Almost all of the researchers investigating the effects of boriding on the friction coefficient concluded that boriding reduces the friction coefficient [25,26].

Growth kinetics of boride layer is specified by the depth measurement of FeB and Fe₂B layers as a function of boriding time and temperature. There is no simple relationship between surface and interface morphology. Fe₂B columnar structure at the material interface is explained with the growth mechanism from the end. While Fe₂B grows inside the soft material, FeB grows inside the hard Fe₂B matrix and thus different local stresses and interface deteriorations occur. Borides are non-oxide ceramics and mostly brittle.

The effects of Ekabor-2 bath on the formation mechanism and the properties of the boride layer in the boriding by thermo-chemical diffusion method of AISI 316L stainless steel were investigated in this study. Different temperatures and times were applied in boriding operations. Various experiments were carried out after the boriding process to detect the properties of the boride layers.

The character of the boride layer surface was observed by optical microscope; phases formed were detected by X-ray diffraction method; the character of boride layer was detected by electron probe micro analyzer (EPMA) and boride layer morphology was investigated by scanning electron

microscope (SEM) and EPMA. Coating thickness values were measured and furthermore, hardness profile of the borided surface was obtained.

2. EXPERIMENTAL METHOD

Hot rolled and annealed AISI 316L austenitic stainless steel was used in boriding processes. The composition of this steel is given in Table 1. The proper specimens were prepared from the stainless steel sheet for experimental studies.

Table 1. The chemical composition of AISI 316L stainless steel materials used in the experimental studies.

Element	C	Si	Mn	P	S	Cr	Ni	Mo	N
% wt.	0.015	0.45	1.50	0.026	0.028	16.98	10.2	2.07	0.07

Boriding operations were carried out in commercial Ekabor-2 boriding bath under argon atmosphere and small AISI 304 stainless steel containers were used in the boriding. Experiments were performed at 850, 950 and 1050°C for 2, 4 and 6 hours, taking into account the accepted temperatures and times in the literature.

Athmospheric-controlled Heraeus branded electric resistance furnace was used for boriding the specimens. Specimens were air cooled down to room temperature and residues on the specimen surfaces after boriding process were removed by holding the specimens in the boiling water. Then the specimens were exposed to ultrasonic cleaning in the alcohol.

Hardness measurements of boride layer and substrate of borided specimens were carried out by Future Tech FM 700 branded microhardness tester with a Vickers indenter under a load of 0.1 N. Hardness measurements were conducted from the surface to the substrate in certain intervals. Thus the change in the hardness from surface to the substrate was detected depending on the bath composition, boriding temperature and time. Hardness values were measured for all temperatures and times.

Boride layer thickness measurements were carried out using layer thickness detection methods developed for boriding. Computer-controlled Nikon Epiphot 200 branded optical microscope having Clemex image analysis program was used to examine the specimens. The zone from the outer surface to the end part was chosen as layer thickness and the average of 10 measurements were calculated and noted as layer thickness. Equation 1 developed first by Brakman [27] which is a special analysis of Fick's law was utilized for the calculation of diffusion coefficient in the boride structure of boron during the investigation of boride layer thickness in terms of kinetics. There is an exponential relationship between diffusion coefficient (D) which is a measure for displacement trend of boron atoms and temperature (Eq. 1). Diffusion coefficient is a property unique to material and sets the rate of diffusion.

$$d^2 = D t \tag{1}$$

Here; d is layer thickness (cm), D is diffusion coefficient (m^2s^{-1}), t is time (s). Activation energy required for the formation of the coating layer (Q) and Frequency factor (D_0) values were found from the Arrhenius equation (Eq. 2).

$$D = D_0 \exp(-Q/RT) \quad (2)$$

Here, D_0 is frequency factor (m^2s^{-1}), Q is activation energy (Jmol^{-1}), R is gas constant ($8.3145 \text{ Jmol}^{-1} \text{ }^\circ\text{K}$), and T is temperature ($^\circ\text{K}$).

Activation energy required for the boride layer formation and diffusion coefficient values of boron were found depending on the boride layer thickness of borided specimens after the calculations.

X-ray diffraction method (XRD) was used to detect the phases formed on the surfaces of borided specimens. PHILIPS PW 3710 branded X-ray diffractometer and JADE Materials Data XRD Pattern Processing V5.0.2195(2) Service Pack 2 and ICDD database and $\text{Co K}\alpha$ ($\lambda = 1.79021 \text{ \AA}$) radiation source and 2θ angles ranging from 10 to 90° were used.

Studies on the Secondary Electron (SE) and Back Scattered Electron (BSE) images, X-ray mapping and detection of the chemical composition of boride layer were made by electron probe micro analyzer (EPMA) instrument. Scanning electron microscope (SEM) was used to investigate the properties of the boride layers. SEM and elemental diffusion spectrometry (EDS) analyses were carried out by JEOL JSM T-330 and JEOL-JSM5410 scanning electron microscopes.

3. RESULTS AND DISCUSSION

Boride layer thicknesses of specimens borided at 850 , 950 and 1050°C for 2 , 4 and 6 h were measured and layer thickness values depending on the boriding time were given in Table 2.

Table 2. Layer thickness values depending on boriding temperature and time.

Boriding temperature ($^\circ\text{C}$)	Boriding time (h)	Layer thickness (μm)
850 $^\circ\text{C}$	2	9.8
	4	16.9
	6	20.1
950 $^\circ\text{C}$	2	12.7
	4	24.9
	6	41.4
1050 $^\circ\text{C}$	2	23.3
	4	38.1
	6	60.9

Micrographs showing the boride layers of metallographically prepared sections of borided specimens at 850 °C and 1050°C for 6 h were given in Figure 1 (a) and (b) respectively. Boride layer thickness was found to increase with the boriding temperature. Different structures from the surface were observed depending on the boriding temperature and time after boriding process. These are;

- (a) Boride layer zone containing the boride phases in its composition in the form of compact and flat layer,
- (b) Boron-rich transition zone having a grain structure different from the matrix,
- (c) Steel matrix.

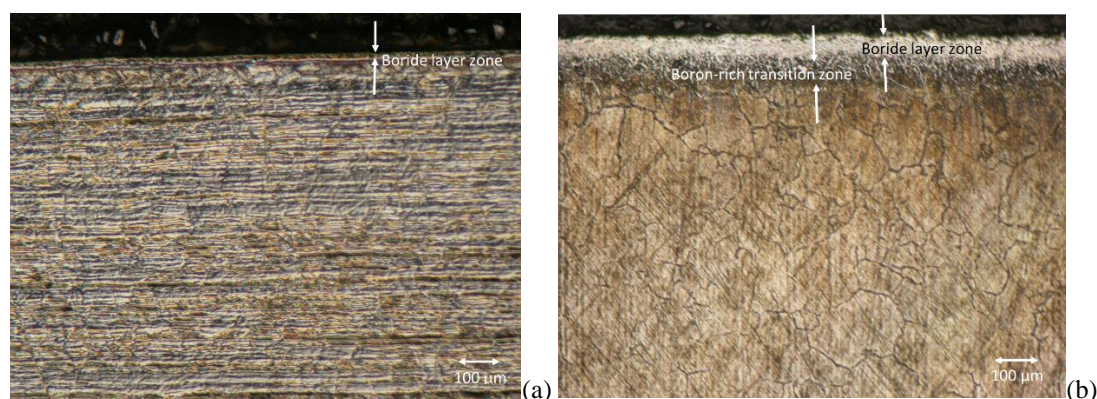


Figure 1. Cross-sectional views of borided specimens at 850°C (a) and 1050°C (b) for 6h.

In Figure 1a, the boron-rich transition zone cannot be seen clearly because the boriding temperature is not very high. It is pointed out in many studies that boride layer formed in the tooth-like form in the pure iron and plain carbon steels [28], and formed in the form of plain-like -not in the form of tooth-like- in the alloyed steels depending on the alloying elements [29-30]. It is seen that the coating thickness obtained for boriding at 850°C for 2 h is 9.8 µm. The highest coating thickness was reached in boriding at 1050°C for 6 h and the obtained coating thickness value was 60.9 µm. It is also seen that similar coating thicknesses were obtained in a boriding study [30] performed on AISI 316L steel with Ekabor-2 (6.2 – 63.5 µm). It is reported that the coating thickness obtained in another study, in which continuous boriding was performed on AISI 316L stainless steel with Ekabor-2 at 900°C for 1 h, was approximately 13 µm [31].

There are theoretically two factors in growth reaction kinetics. These are reaction products diffused on the reaction interface (diffusion-controlled) and a chemical barrier for transportation of the substances reacting on the reaction interface (reaction controlled). Boride layer grows linearly as the treatment time increases in the case of reaction-controlled process; it grows proportional to the square root of the reaction time if the process is diffusional. The increase in the layer thickness depending on the time and temperature is an expected result since boriding process is a diffusional process.

Although boride layer thicknesses formed in the boriding process are homogeneous on all over the specimen surface, some differences are observed in the length of the boride columns. The reason for these differences is the occurrence of boron gradient from the surface being enriched with boron to the substrate [32,33]. Contour diagram showing the boride layer depth depending on the temperature and time is shown in Figure 2. This diagram provides an ease of estimation for tuning the boriding process parameters in the industry.

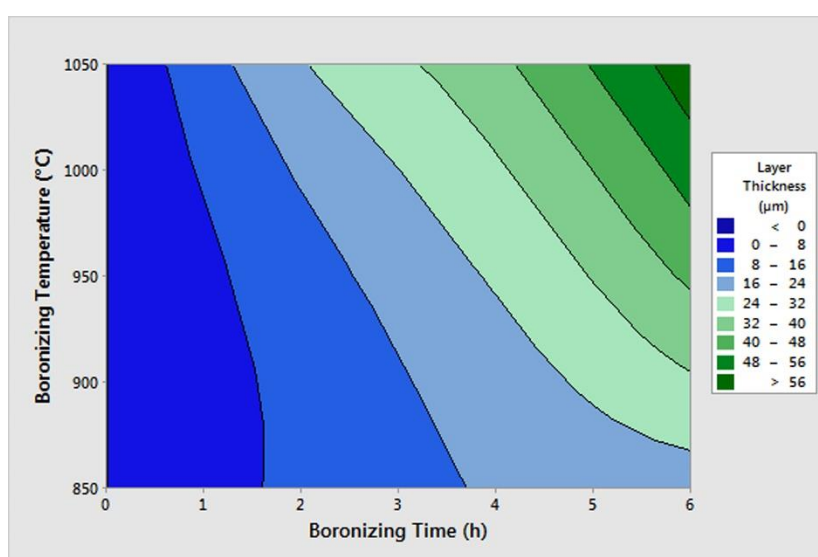


Figure 2. Contour diagram showing the layer thickness depending on the temperature and time.

3.1. Investigation of Boride Layer Thickness in Terms of Kinetics

Diffusion coefficient of boron in the boriding treatment were calculated by Eqs. 1 and 2 (developed by Brakman) utilizing the diagrams belonging to the boride layer thicknesses depending on the boriding time and temperature. Diffusion coefficients were calculated from the slope of d^2-t diagrams shown in Figure 3 and given in Table 3 for the borided specimens.

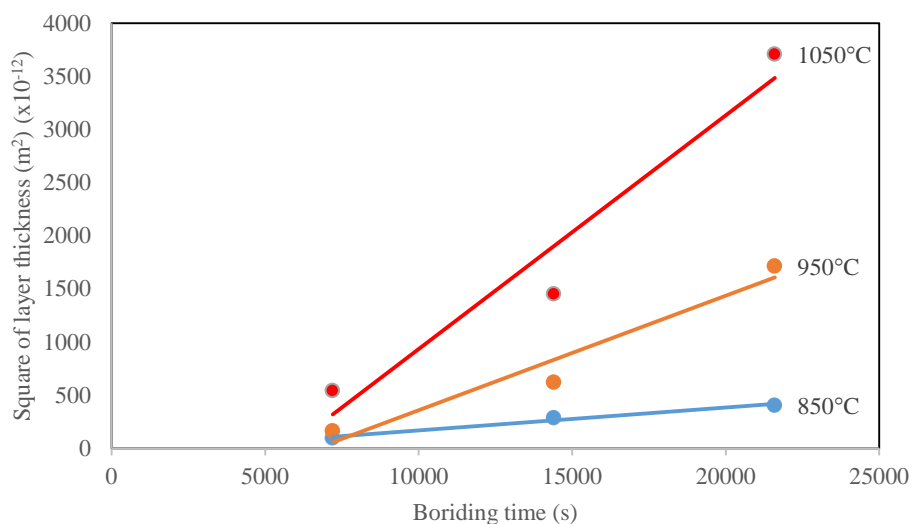


Figure 3. Variation of square of the boride layer thickness with time for different temperatures on the borided specimens ($d^2 - t$ variation).

Table 3. Diffusion coefficients of boron depending on the temperature during boriding treatment.

Temperature (°C)	Diffusion coefficient (m^2s^{-1})
850	2×10^{-14}
950	11×10^{-13}
1050	22×10^{-13}

Activation energy for the occurrence of boride layer was found using the diffusion coefficients and $\ln D - 1/T$ curve was drawn according to the Arrhenius equation and shown in Figure 4. There is an exponential relationship between temperature and the diffusion coefficient (D) which is a measure for the displacement trend of the atoms.

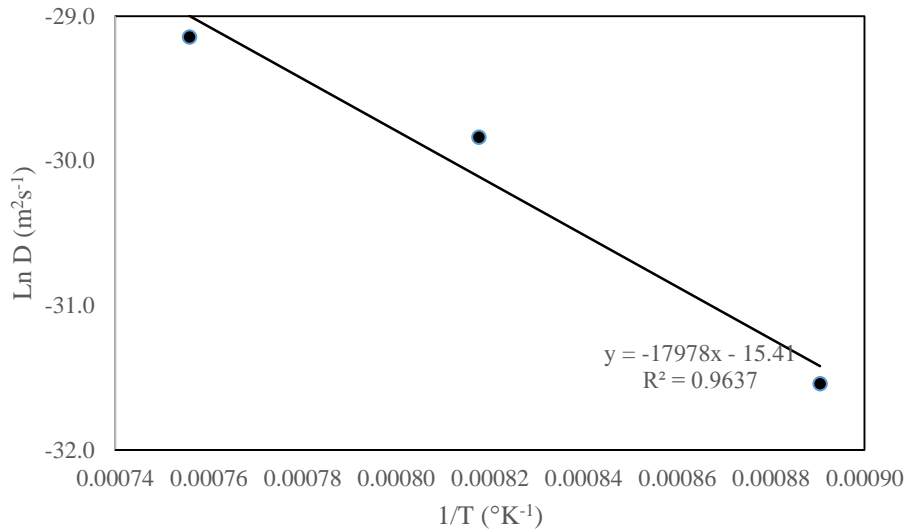


Figure 4. Variation of diffusion coefficient with the inverse of temperature.

Activation energy and frequency factor values of boride layer are given in Table 4. Diffusion coefficient is a unique property for the material and also governs the diffusion rate. Activation energy decreases as the diffusion coefficient increases and thus the diffusion rate increases. Desired layer thicknesses can be estimated practically without performing any experiments for a certain temperature and time after obtaining these kinetic data (Q , and D_0). Practical equations seen below (Eq. 3) were deduced for the calculation of diffusion coefficients from the kinetic data found in this study.

Table 4. Activation energy (Q) and frequency factor (D_0) values of boride layers.

Bath	Q (kJmol ⁻¹)	D_0 (m ² s ⁻¹)
Ekabor-2	149.3	1.96×10^{-7}

Diffusion coefficient of boron for borided AISI 316L steel specimen:

$$D = 1.96 \times 10^{-7} \exp(-17978/T) \quad (3)$$

Bath compositions utilized in the kinetic study are effective on the diffusion coefficient and activation energy values found in this study. Bozkurt and Sundararajan [34,35] point out the effect of boriding media and material composition on the kinetic values found in their studies on the steels. Activation energy results of some boriding studies made by different boriding methods were given in Table 4. Activation energies for the formation and growth of boride layers are consistent with the literature as can be seen from Table 5 [30,31,36-45].

Table 5. Activation energy values in some boriding studies carried out by different boriding methods.

Boriding Method	Material	Conditions (Temperature ; time)	Activation Energy (kJmol⁻¹)	Hardness (HV)	Ref. No
Salt bath: Ekabor-2	AISI 316L	850,950,1050° C; 2,4,6 h	149.3	1543-1795	-
Salt bath: Ekabor-2	AISI 316L	800,850,900,950° C; 2,4,6 h	244.15	2125 (max)	[30]
Salt bath: Ekabor-2	AISI 316L	900°C; 1 h		26,3 (GPa)	[31]
Salt bath: Ekabor	AISI 316	800,875,950° C; 2,4,6,8 h	199.0	1700	[36]
Salt bath: 65% borax, 15% boric acid, %20 FeSi	AISI 4140	850,900,950° C; 2,4,6,8 h	215.0	1446-1739	[37]
Salt bath: borax and boric acid, FeSi	AISI 5140	850,900,950° C; 2,4,6,8 h	223.5	1198-1739	[38]
Salt bath: borax and boric acid, FeSi	AISI 4340	850,900,950° C; 2,4,6,8 h	233.7	1077-1632	[38]
Vacuum boriding: boron powder (98.3% B, 0.04% C, 1.6% O, 0.01%>Si-Cu-Mg, 0.001>Fe), Activator KBF ₄	Fe-%10 Cr	850,900, 950°C; 1-12 h	147.5 (156.4 FeB ₂)	1180-1300	[39]
Salt bath: Ekabor-2 (90% SiC, 5% B ₄ C, 5% KBF ₄)	AISI 440C	950°C; 2 h		2160	[40]
Salt bath: 60% borax, 20% boric acid, 20% FeSi	AISI 304	800,950°C; 3,5,7 h		2150	[41]
Salt bath: 70% borax, 30% SiC	AISI 316L	850,950,1000° C; 2,4,6 h	174.6		[42]
Salt bath: Ekabor-2	AISI D2 AISI M2	950°C; 1h 1000°C; 1h		2000 2000	[43]
Salt bath: Ekabor-2	ASTM A36	850,900,950, 1000°C 2,4,6, 8 h	161		[44]
Boron powder (Hef-Durferrit)	80/20 Ni-Cr	900,950,975° C; 2,4,6 h	145,9	1052-1350	[45]

3.2. X-Ray Diffraction Results

The results of X-ray diffraction analyses of the phases formed on the boride layers of specimens which were borided at 1050°C for 6 h are given in Figure 5 as an example. It is seen from the X-ray diffraction analysis graphics that FeB phase peaks in addition to Fe₂B phase are present in the layer formed in the borided specimens.

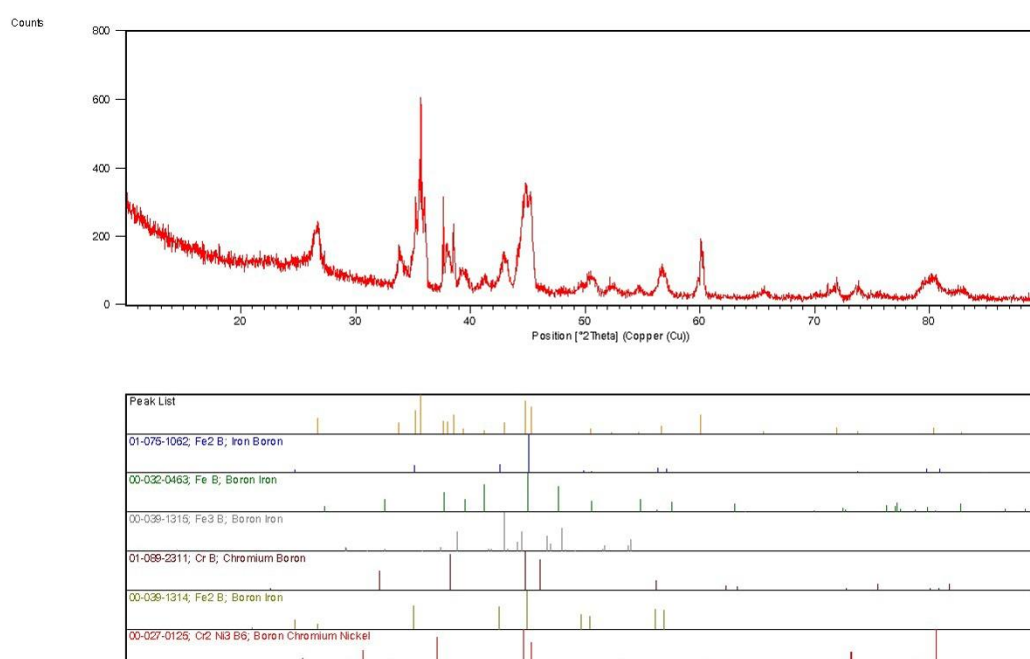


Figure 5. The results of X-ray diffraction analyses of the phases formed on the boride layers of specimens which were borided at 1050°C for 6 h.

SE and BSE images obtained from the EPMA and SEM investigations belonging to the boride layers of borided specimens are given in Figure 6; elemental distribution images obtained from X-ray mapping are given in Figure 7. Boride layer thickness is almost the same on all over the specimen as seen in Figure 6: boride layer formed homogenously on the surface. However, it is observed that there have been differences in the length of boride columns. The differences in the length of columns result from the boron gradient (concentration difference) between boron-enriched surface and substrate [32,33]. Boride layers, layer-substrate transition zone and substrate are obviously observed from the investigation by SEM and EPMA of boride layer morphologies of borided specimens. After the boriding process following structures and zones were observed depending on the boriding temperature and time: i) non-metallic ceramic zone in the form of compact and flat layer containing boride phases,

- ii) metallic transition zone between boride layer and matrix in which the boron concentration decreases from the surface; and this zone is non-homogeneous and poorer than the surface as boron,
- iii) structures in the form of matrix in the original material's structure unaffected by the boriding.

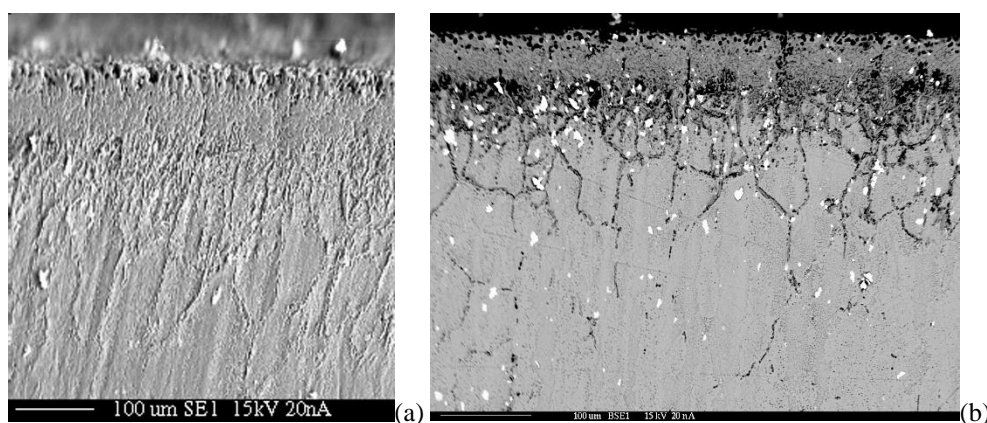


Figure 6. Images of boride layers formed on the AISI 316L stainless steel specimens borided at 1050°C for 6 h: (a) SE image, (b) BSE image.

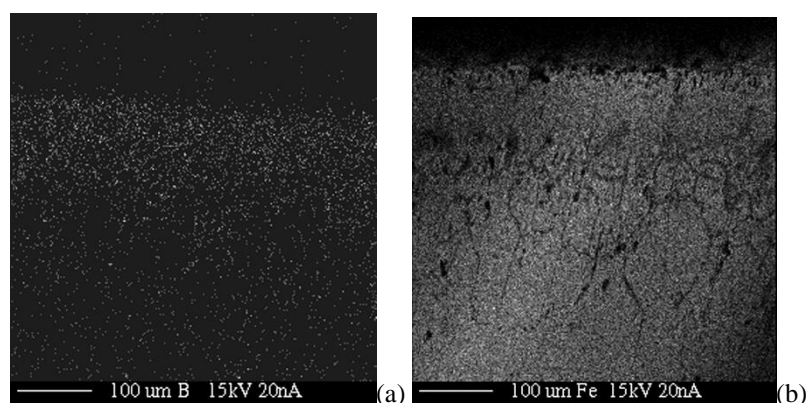


Figure 7. The X-ray mapping images of B and Fe on the surface of boride layers formed on the AISI 316L stainless steel specimens borided at 1050°C for 6 h: (a) B, (b) Fe.

Boride structure was observed to be in the form of a flat layer depending on the Cr, Ni and Mo content of stainless steel. Boride layer forms in tooth-shape structure in the pure iron and plain carbon steels [28]. Boride layer forming depending on the alloying elements in the alloyed steels is in the form of smooth structure more than the tooth-shape structure [29]. Also alloying elements in the investigated AISI 316L stainless steel made boride layer smooth. B content was observed to be 2.085% at the

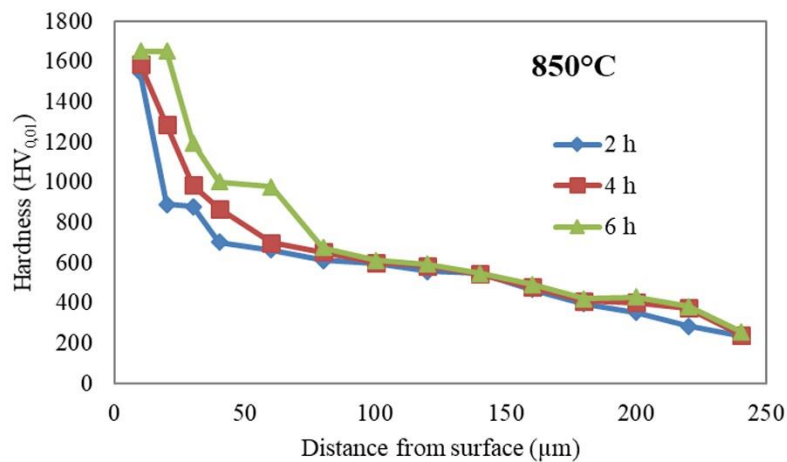
middle zone of the sections of boride layers of specimens borided at 1050°C for 6 h by semi-quantitative analysis method.

3.3. Hardness Results

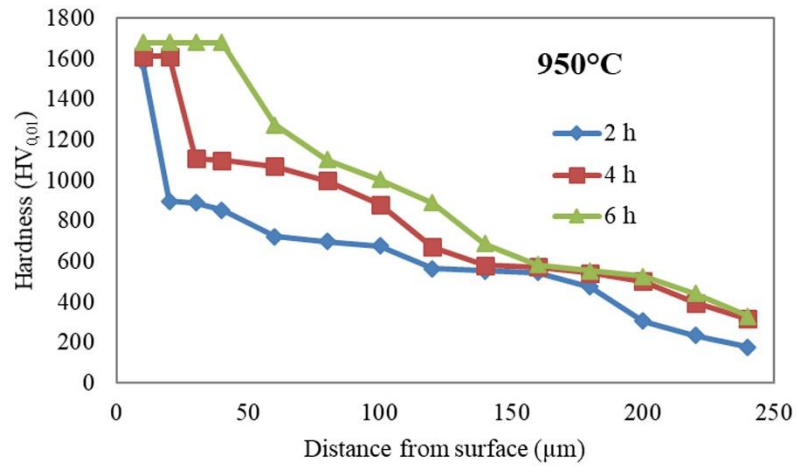
Hardness measurements were carried out on the borided specimens at certain distances from surface to the substrate. By this way, variation of the hardness from surface to substrate was observed depending on the boriding time and temperature. Hardness measurements were performed for all temperature and time conditions.

Hardness distribution of the materials borided at 850, 950, and 1050 °C for 2, 4, 6 h were given in Figure 8. Hardness values gradually decrease in the specimens borided at 850°C for all boriding times depending on the distance from the surface as can be seen from Figure 8 (a). The highest hardness was obtained in the regions near the surface, and being the richest zone in terms of boron. Hardness values were also found to increase with the increasing time. The hardness values seem to keep the high values on the surface toward the interior as the boriding temperature increased especially for the boriding time of 6h. The surface hardness value appears to be maintained up to 60µm at boriding temperature of 1050°C for 6h (Figure 8 (c)).

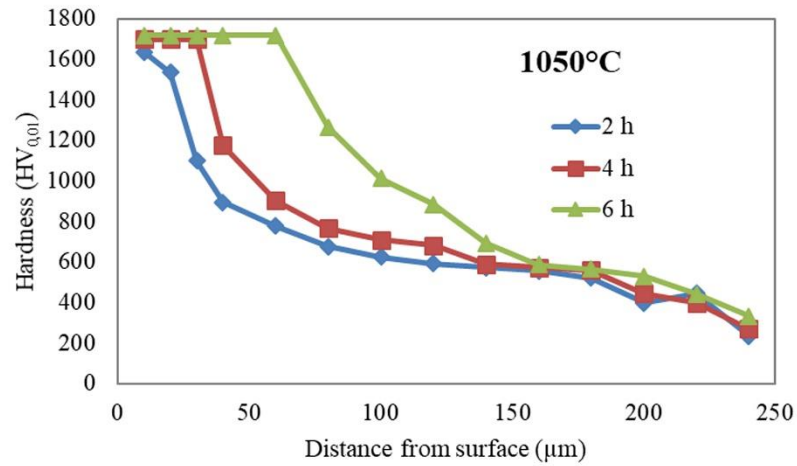
Surface hardness values of borided materials increase depending on the temperature and time. The hardness of non-borided AISI 316L stainless steel specimen is HV170. Surface hardness values of borided materials are 9.1 to 12 times higher than the non-borided material depending on the temperature and time. Taktak [41] has found that surface hardness values of borided AISI 304 stainless steel were 7.4 to 11 times higher depending on the temperature and time than the non-borided one.



(a)



(b)



(c)

Figure 8. Hardness distribution of borided specimens at (a) 850°C, (b) 950°C, (c) 1050°C for 2, 4 and 6 h.

Surface hardness values obtained in this study and some values from the literature are seen in Table 5. Basic phase in the boride layer formed in the boriding is Fe₂B. FeB phase also forms.

4. CONCLUSIONS

The following results were obtained in the studies on boriding the surfaces of AISI 316L stainless steel material with Ekabor-2.

The thickness of boride layer increases with the increasing temperature and time during the boriding process.

Boride layers which form on the surfaces of the specimens are continuous and have a smooth structure. The basic phase in the boride layer formed in the boriding processes of stainless steel is Fe₂B. FeB phase also formed in the boriding with the bath containing Ekabor-2.

Activation energy for the formation and growth of boride layer is 149.319 kJmol⁻¹ in the boriding with the bath containing Ekabor-2 and consistent with the literature.

Surface hardness values of borided materials increase during the boriding process depending on the temperature and time.

ACKNOWLEDGEMENT

The authors acknowledge Yılmaden Holding, Eti Krom A.Ş. R&D Center.

REFERENCES

- [1] Güven, Ş.Y., (2014), Biyouyumluluk ve biyomalzemelerin seçimi. Süleyman Demirel University, Journal of Engineering Sciences and Design, 2(3) SI:BioMechanics, 303-311.
- [2] Güven, Ş.Y. and Delikanli, K., (2006 Nisan), Metalik biyomalzemelerde son gelişmeler. TİMAK-Tasarım İmalat Analiz Kongresi, Balıkesir, 26-28.
- [3] Patel, N.R. and Gohil, P.P., (2012), A review on biomaterials: Scope, applications and human anatomy significance. International Journal of Emerging Technology and Advanced Engineering, 2(4), 91-101.
- [4] Geetha, M., Singh, A.K., Asokamani, R. and Gogia, A.K., (2009), Ti based biomaterials, the ultimate choice for orthopaedic implants - A review. Progress in Materials Science, 54, 397-425.
- [5] Paital, S.R. and Dahotre, N.B., (2009), Calcium phosphate coatings for bio-implant applications: Materials, performance factors, and methodologies. Materials Science and Engineering R, 66, 1-70.

- [6] Talha, M., Behera C.K. and Sinha, O.P., (2013), A review on nickel-free nitrogen containing austenitic stainless steels for biomedical applications. *Materials Science and Engineering C*, 33(7), 3563–3575.
- [7] Arsiwala, A., Desai, P. and Patravale, V., (2014), Recent advances in micro/nanoscale biomedical implants. *Journal of Controlled Release*, 189(10), 25–45.
- [8] Parsapour, A., Khorasani, S.N. and Fathi, M.H., (2012), Effect of surface treatment and metallic coating on corrosion behavior and biocompatibility of surgical 316L stainless steel implant. *Journal of Materials Science and Technology*, 28(2), 125–131.
- [9] Rautray, T.R., Narayanan, R. and Kim, K-H., (2011), Ion implantation of titanium based biomaterials. *Progress in Materials Science*, 56(8), 1137–1177.
- [10] Chen, Q. and Thouas, G.A., (2015), Metallic implant biomaterials. *Materials Science and Engineering R*, 87(1), 1–57.
- [11] Tiwari, S.K., Mishra, T., Gunjan, M.K., Bhattacharyya, A.S., Singh, T.B. and Singh, R., (2007), Development and characterization of sol–gel silica–alumina composite coatings on AISI 316L for implant applications. *Surface & Coatings Technology*, 201, 7582–7588.
- [12] Schwab, H., Prashanth, K.G., Löber, L., Kühn, U. and Eckert, J., (2015), Selective laser melting of Ti-45Nb alloy. *Metals*, 5, 686-694.
- [13] Lemons, J.E., Misch-Dietsh, F. and McCracken, M.S., (2015), Biomaterials for dental implants, In *Dental Implant Prosthetics* (pp. 66-94). Elsevier Inc.
- [14] Öztürk, O., (2009), Microstructural and mechanical characterization of nitrogen ion implanted layer on 316L stainless steel. *Nuclear Instruments and Methods in Physics Researchs Section B: Beam Interactions with Materials and Atoms*, 267(8-9), 1526–1530.
- [15] Başman, G. and Şeşen, M.K., (2011), AISI 316 L tipi paslanmaz çeliğin yüzey özelliğinin borlama ile geliştirilmesi. *İTÜ Dergisi/D Mühendislik*, 10(2), 115-121.
- [16] Sinha, A.K., (1991), Boriding (Boronizing), *ASM Handbook, J. Heat Treatment*, OH, USA, 4, 437-447.
- [17] TMMOB Metalurji Mühendisleri Odası, Bor Raporu, (2003), *Metalurji Dergisi*, 134, 11-72.
- [18] Hocking, M.G., Vasantasree, V. and Sidky, P.S., (1989), *Metallic and ceramic coatings*. John Wiley & Sons Inc., New York, pp. 1-2.

- [19] Yapar, U., Başman, G., Arısoy, C.F., Yeşilçubuk A., and Şeşen, M.K., (2004), The influence of boronizing on mechanical properties of EN-C35E steel, *Key Engineering Materials*, 264-268, 629-632.
- [20] Matuschka, A.G., (1980), *Boronising*. Carl Hanser Verlag, München.
- [21] Graf, A. and Matuschka, W., (1997), *Borieren*. Carl Hanser Verlag, München, Wien, pp.1-87.
- [22] Yapar, U., Arısoy, C.F., Başman, G., Yeşilçubuk S.A. and Şeşen, M.K., (2004), Surface modification of EN-C35E steels by thermochemical boronizing process and its properties, *Key Engineering Materials*, 264-268, 633-636.
- [23] Ficht, W., Trausner, N. and Matuschka, A.G., (1987), *Borieren mit ekabor*, ESK GmbH.
- [24] Eyre, T.S., (1975), Effect of boronising on friction and wear of ferrous metals. *Wear*, 34, 383-397.
- [25] Geoeuriot, P., Thevenot, F., Driver, J.H. and Magnin, T., (1983), Methods for examining brittle layers obtained by a boriding surface treatment (Borudif). *Wear*, 86, 1-10.
- [26] Soydan, Y., (1996), Katı ortamda bor yayılımı ile sertleştirilen çelik yüzeylerinin kuru kayma halinde sürtünme ve aşınma davranışları, Doktora Tezi, İ.T.Ü. Fen Bilimleri Enstitüsü, İstanbul.
- [27] Brakman, C.M., Gommers, A.W.J. and Mittemeijer, E.J., (1989), Boriding of Fe and Fe-C, Fe-Cr, and Fe-Ni Alloys: Boride layer kinetics. *Journal of Materials Research*, 4, 1354-1370.
- [28] Palombarini, G. and Carbucicchio, M., (1984), On the morphology of thermochemically produced Fe₂B/Fe interfaces. *Journal of Materials Science Letters*, 3, 791-794.
- [29] Carbucicchio, M. and Palombarini, G., (1987), Effects of alloying elements on the growth of iron boride coatings. *Journal of Materials Science Letters*, 6, 1147-1149.
- [30] Ayvaz, S.I. and Aydın, I., (2020), Effect of the microwave heating on diffusion kinetics and mechanical properties of borides in AISI 316L. *Transactions of the Indian Institute of Metals*, 73(10):2635-2644.
- [31] Valdes, D.F., Rosa, O.V.D., Castro, G.A.R., Amador, A.M., Lievano, A.L., Ramírez, A.O., (2021), *Surface & Coatings Technology*, 423, 127556, 1-11.
- [32] Başman, G., (2010), AISI 316L tipi paslanmaz çeliğin termokimyasal difüzyon yöntemi ile borlanması, borlama banyosu bileşenlerinin borür tabakası özelliklerine etkisi, Doktora tezi, İ.T.Ü. Fen Bilimleri Enstitüsü, İstanbul.

- [33] Yapar, U., (2003), Düşük ve orta karbonlu çeliklerin termokimyasal borlama ile yüzey özelliklerinin geliştirilmesi, Yüksek Lisans Tezi, İ.T.Ü. Fen Bilimleri Enstitüsü, İstanbul.
- [34] Bozkurt, N., (1984), Bor yayınımla çeliklerde yüzey sertleştirme, Doktora Tezi, İ.T.Ü. Fen Bilimleri Enstitüsü, İstanbul.
- [35] Chen, X.J., Yu, L.G., Khor, K.A. and Sundararajan, G., (2007), The effect of boron-pack refreshment on the boriding of mild steel by the spark plasma sintering (SPS) process. *Surface & Coatings Technology*, 202(13), 2830–2836.
- [36] Ozdemir, O., Omar, M.A., Usta, M., Zeytin, S., Bindal, C. and Üçışık, A.H., (2009), An investigation on boriding kinetics of AISI 316 stainless steel. *Vacuum*, 83, 175–179.
- [37] Şen, Ş., Şen, U. and Bindal, C., (2005), The growth kinetics of borides formed on boronized AISI 4140 Steel. *Vacuum*, 77, 195-202.
- [38] Şen, Ş., Şen, U. and Bindal, C., (2005), An approach to kinetic study of boride steels. *Surface & Coatings technology*, 191, 274-285.
- [39] Dybkov, V.I., Lengauer, W. and Barmak, K., (2005), Formation of boride layers at the Fe-%10Cr alloy-boron interface. *Journal of Alloys and Compounds*, 398(1-2), 113,122.
- [40] Taktak, Ş., (2006), Tribological behavior of borided bearing steels at elevated temperatures. *Surface & Coatings Technology*, 201(6), 2230-2239.
- [41] Taktak, Ş., (2007), Some mechanical properties of borided AISI H13 and 304 steels. *Materials Design*, 28(6), 1836-1843.
- [42] Mebarek, B., Madouri, D., Zanoun, A. and Belaidi, A., (2015), Simulation model of monolayer growth kinetics of Fe₂B phase, *Materiaux and Techniques*, 103(7), 703.
- [43] Ertürk, Ş. and Kayabaşı, O., (2019), Investigation of the cutting performance of cutting tools coated with the thermo-reactive diffusion (TRD) technique. *IEEE Access*, 7, 106824-106838.
- [44] Ortiz-Domínguez, M., Gómez-Vargas, O.A., Ares de Parga, G., Torres-Santiago, G., Velázquez-Mancilla, R., Castellanos-Escamilla, V.A., Mendoza-Camargo, J. and Trujillo-Sánchez, R., (2019), Modeling of the growth kinetics of boride layers in powder-pack borided ASTM A36 steel based on two different approaches. *Advances in Materials Science and Engineering*, 2019-7.
- [45] Ulloa A.C, Trabolsi, P.A.R., Avila, I.P.T., Álvarez, C.O., Rosas, R.T., Velázquez, J.C. and Sánchez, E.H., (2022), Kinetics and mechanical characterization of hard layers obtained by boron diffusion in 80/20 nickel–chromium alloy. *Coatings*, 12, 1387, 1-14.